

# Development of a lifetime model for VRLA batteries used in wind turbine generators

XL Wang\*, SS Choi\*, TL Zhang\*\* and KJ Tseng\*

\*School of Electrical and Electronic Engineering

Nanyang Technological University, Singapore

\*\* Vestas Technology R&D Center, Singapore

**Abstract:** An approach to predict the remaining lifetime of lead-acid battery is described. The battery is used to provide back-up power to keep essential devices within wind turbine generators operational under emergency conditions. The approach is developed from a circuit model of the battery. From the results of laboratory tests, changes in the model parametric values due to ambient temperature variations, battery aging effects as well as discharge current level have been quantified. Through a developed computational method, the terminal voltage and state of charge of the battery at any other discharging conditions can then be calculated. The discharge profile allows one to predict the remaining lifetime of the battery. The predicted results appear to agree most satisfactorily with that obtained from laboratory measurements.

**Keywords:** Back-up power supply, lead-acid battery, state of discharge, lifetime prediction.

## 1 INTRODUCTION

Battery has become a crucial component of many electrical systems, and the prediction of its useful lifetime is very important for technical and commercial reasons. Lifetime prediction can be used to select the most suitable battery, to determine the operating conditions and to plan replacement schedule [1, 2].

There are many stress factors, such as ambient temperature, charge factor and partial cycling, which induce battery aging and influence the aging rate [3]. These factors should be considered in any attempt to obtain accurate lifetime prediction. Usually, in practice, there exist complex combinations of these stress factors along with large variations of the operational condition in applications. In view of this and with only finite amount of field results and observations, building a model which can be used to predict battery lifetime for all applications is very challenging because the results of prediction depend on the actual application condition.

On the other hand, if a battery model can be constructed to describe the battery behavior for a specific application, the modeling and corresponding analysis can be done by focusing mainly on those dominant stress factors affecting the lifetime. In this manner, the modeling process for lifetime prediction can be simplified and the prediction can be made with reasonable confidence level. It is in this consideration that the present investigation was initiated.

A summary of some of the conventional battery lifetime prediction models is given in Section 2. The

main objective of this investigation is to develop an approach to predict the lifetime of a specific type of valve-regulated lead-acid (VRLA) batteries. This approach is described in Section 3, in which experimental tests are used to emulate as closely as possible the operating condition of the batteries under specific application in wind turbine generators (WTG). In the experiments described in Section 4, the performance of the batteries which have undergone accelerated aging process was measured using a developed data acquisition system and software tool. The effects of some of the prominent stress factors on the battery performance are represented by circuit elements, the values which are determined from the test measurements. This is included in Section 5. Based on the circuit model, the battery performance can then be estimated for different operating conditions and from which the lifetime of the battery can be inferred. Details of this are presented in Section 6.

## 2 CONVENTIONAL BATTERY REMAINING LIFETIME PREDICTION METHODS

To predict the battery lifetime, a proper battery model must be obtained. Since the late 1950s, many VRLA battery models have been proposed by researchers, see e.g. [4 – 11]. Essentially, the models can be classified into the two main types: post-processing models and performance degradation models. The two types of models also differ in the way of their requirements for data.

The post-processing models link the end-of-life of a battery to some parameters which can be easily determined, e.g. amp-hour (A-h) throughput. Data required by post-processing models is generally available from the battery manufacturers. On the other hand, the data required by the performance degradation models have to be acquired by conducting measurements on tests which emulate as closely as possible the battery working conditions.

The main causes of VRLA battery deterioration in performance can be divided into two main categories, depending on usage mode. One is due to floating service and the other is cycle use [12]. The VRLA battery examined in this investigation is to operate under floating-charge mode in WTG. Hence, only lifetime deterioration of the battery under floating-charge mode shall be examined. During floating service, the main cause of deterioration is positive grid corrosion which is known to be dependable strongly on the battery ambient temperature. Also, higher ambient temperature will cause more water loss. Thus, the battery life will decrease with an increase in ambient temperature [12].

Indeed, typically the lifetime of a VRLA battery will be halved for every 10°C rise in ambient temperature [12]. Thus the equivalent lifetime  $L_X$  of the VRLA battery at the given reference temperature of  $X^\circ\text{C}$  can therefore be calculated as

$$L_X = L_T \times 2^{((T-X)/10)} \quad (1)$$

where  $L_T$  is the lifetime of the battery (expressed in years) at an operating ambient temperature of  $T^\circ\text{C}$ .

### 3 AN APPROACH ON THE PREDICTION OF BATTERY REMAINING LIFETIME

In order to predict the remaining lifetime of a battery at the reference temperature of  $X^\circ\text{C}$ , two pieces of information are needed: (a) The total service lifetime of the batteries,  $L_{T,X}$ , and (b) The length of time the battery has been in service, i.e., the so-called equivalent service lifetime  $L_{S,X}$ . The remaining lifetime ( $L_{R,X}$ ) would then be

$$L_{R,X} = L_{T,X} - L_{S,X}. \quad (2)$$

In view of (2), the procedure involved in predicting  $L_{R,X}$  is shown in Fig. 1. Step 1 of Fig. 1 is to calculate the equivalent service lifetime  $L_{S,X}$  of the battery. Suppose the historical ambient temperature of the battery in service is available. The temperature-time data is then sectionized into sub-intervals. In each of the sub-intervals, the ambient temperature  $T$  is considered essentially constant. Using (1), one can then calculate the equivalent lifetime  $L_X$  of the battery for each of the intervals, evaluated at the reference temperature  $X^\circ\text{C}$ . The equivalent service lifetime  $L_{S,X}$  at the reference temperature  $X^\circ\text{C}$  is therefore the sum of all the  $L_X$ .

From (2), however, in order to determine the remaining lifetime  $L_{R,X}$  of the battery, the total service lifetime  $L_{T,X}$  of the battery has to be known too. Step 2 of Fig. 1 shows that there are two possible methods to obtain the total service lifetime, as follows.

#### 3.1 Method based on service life versus temperature

This method, labeled as Method 1 in Fig. 1, is based on the manufacturer's data on expected battery service life versus temperature. Fig 2 shows an example of the relationship between the expected total service lifetime  $L_{T,X}$  and ambient temperature  $X^\circ\text{C}$  of a specific VRLA battery. This relationship is bounded by two limit curves. The upper limit indicates the maximum expected service life of the battery while the lower limit indicates the minimum value. Each of them is a function of the battery ambient temperature. The expected service life of the battery will lie within the shaded area. For lifetime prediction, it is prudent to use the lower limit curve. If the reference temperature is 20°C, for example, the total expected service lifetime is about 9.9 years.

Although this approach is simple, there are severe shortcomings with this method. First, it is not able to account for changes in other operating conditions of the battery, e.g., charging methods and cut-off voltage. The

lifetime prediction result depends on the data supplied by the manufacturers. Usually manufacturers carry out the lifetime test based on certain standard operation conditions. Hence  $L_{T,X}$  provided by the manufacturer is unlikely to be the same as when the battery operates under variable operating conditions, as in WTG.

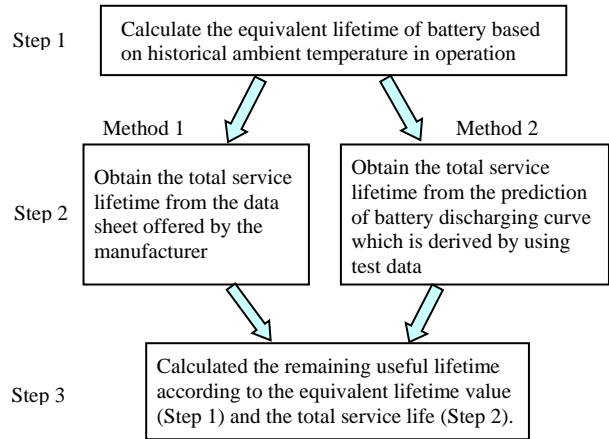


Fig. 1. General procedure for calculating the remaining lifetime  $L_{R,X}$  of a battery

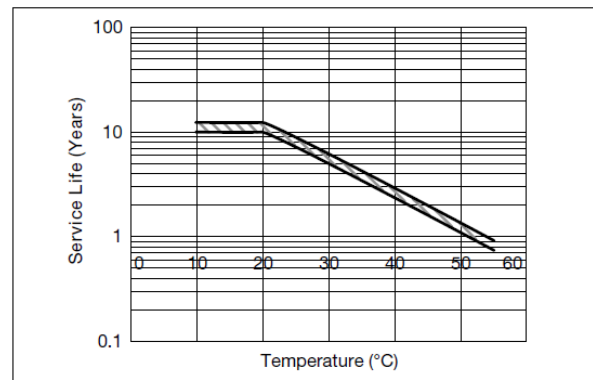


Fig. 2. Battery expected Total Service Lifetime  $L_{T,X}$  versus ambient temperature [5]

#### 3.2 Method based on predicted battery performance

In this investigation, Method 1 is complemented by Method 2 which is based on battery performance prediction. Very often, battery performance is calibrated against the conditions when the battery discharges and reaches a pre-specified minimum terminal voltage. The battery is considered to have come to the end of its useful life if it is unable to maintain the terminal voltage above the minimum value beyond a pre-specified time. The proposed method labeled as Method 2 in Fig. 1 is to predict the  $L_{T,X}$  of the battery when the battery can just meet the minimum voltage condition at the pre-specified time. The remaining lifetime of the battery can then be calculated using (2).

Unlike Method 1, Method 2 has to rely on data obtained from the battery discharge tests. In this way, the results obtained by Method 2 can take into account any other factors, apart from ambient temperature, which may affect the battery performance. The factors may include charging method and the discharge profile.

Hence the results obtained from this method could closely reflect the actual operating condition of the battery. In fact, in order to extend the applicability of Method 2 to account for the variable operational conditions, the battery circuit model shown in Fig. 3 is adopted.

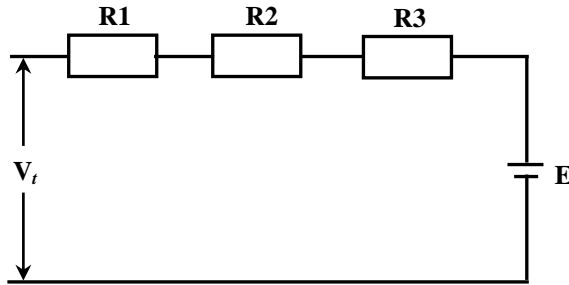


Fig. 3. Battery circuit model adopted in the study

Fig. 3 shows that there are four circuit elements used to represent the battery. In the figure, E is the open circuit voltage of the battery. E is assumed un-affected by the operating conditions and remains constant during a discharge process. This assumption is supported by the results of test measurements which shall be shown in Section 5.

R1, R2 and R3 are three resistances associated with the model. R1 is to account for the change in the discharge performance due to the differences in the discharge current level. R2 is to reflect the change in discharge performance due to the differences in ambient temperature. R3 is to account for the change in discharge performance caused by the differences between the ages of the batteries.

The values of these resistances can be determined from the data obtained from the discharge tests. Also, the test results (to be shown in Section 5) shall ascertain if these resistances may change with the battery's state of discharge (SOD) and whether these resistances can affect each other.

Step 3 of Fig. 1 calculates the expected remaining life  $L_{R,X}$  which is the difference between the total service lifetime  $L_{T,X}$  and the equivalent service lifetime  $L_{S,X}$ . Note that  $L_{R,X}$  is obtained at the reference temperature  $X^\circ\text{C}$ . Hence, one should take into account the actual temperature ( $T$ ) under which the battery operates. Using (1), the expected remaining life  $L_{R,T}$  of the battery operating at the given temperature  $T$  profile is given by

$$L_{R,T} = L_{R,X} / 2^{((T-X)/10)}. \quad (3)$$

## 4 EXPERIMENTAL TESTS

In conjunction with Method 2 described in Section 3, tests are needed to determine the values of the equivalent circuit parameters shown in Fig. 3.

### 4.1 Batteries under test and test equipment

Each of the VRLA batteries under test is rated 12-volt, 6.8 A-h [13]. Three brand-new units of the batteries

were purchased for the purpose. The following software and equipment were used:

A DC electronic load (CHROMA 63200 series) was utilized in the discharge tests;

A software panel was developed to enable remote control of the electronic load;

National Instruments and LabVIEW program were used for data acquisition and system supervision;

A temperature chamber (type SE-300) was used to achieve accelerated aging of the batteries under floating-charge.

## 4.2 Scope of tests and procedure

There are three stages in the test procedure which allows R1, R2 and R3 to be determined. In the discharge tests, room temperature was set at  $25^\circ\text{C}$ . Although there would be heat generated by the batteries during discharges, it is most unlikely the ambient temperature in the test laboratory shall be significantly affected.

Based on the definitions of the resistances in the circuit model, R2 and R3 do not exist when a brand-new battery (assumed to be in pristine condition) discharges under room temperature. Hence, the determination of R1 value was carried out first on a brand-new battery. In the study, tests with constant discharge current at 1.8A, 2.7A, 3.6A and 4.5A were attempted. In this manner, the impact of the ambient temperature during discharge can be accounted for after the R1 tests have been completed.

Next, R2 values were determined at ambient temperature of  $0^\circ\text{C}$ ,  $15^\circ\text{C}$ ,  $25^\circ\text{C}$ ,  $45^\circ\text{C}$ ,  $55^\circ\text{C}$  and  $60^\circ\text{C}$ . Two discharge current levels of 3.6A and 4.5A were used in this process to determine R2.

Finally, tests were performed for the determination of R3. As mentioned in Section 2, accelerated aging of batteries can occur when batteries operate under an environment of higher ambient temperature during floating-charge mode. Therefore, to emulate the actual battery operating condition in a WTG, one of the three brand-new batteries was placed in the temperature chamber under floating-charge mode for weeks. One set of discharge tests was then performed on the battery, after each week of aging. This is for the purpose of tracking the degradation of the battery performance due to the aging effect. Under the floating-charge at a temperature of  $60^\circ\text{C}$ , the charge voltage was set at 13.66V. This charging voltage level is that suggested in the manufacturer's data-sheet.

## 5 ANALYSIS OF TEST RESULTS

### 5.1 Determination of R1 and R2

A sample of test results for determining R1 and R2 is described as follows.

#### 5.1.1 R1 tests: discharge at various current levels

Fig. 4 shows the battery terminal voltage profile versus the battery SOD when the batteries discharge at selected constant current levels. The voltage decreases progressively as the SOD increases, with larger

discharge current causing the batteries to discharge at a lower voltage. The manufacturer's recommended terminating (cut-off) voltage for the batteries is 10.5 V. As stated earlier, this set of tests were performed using the brand-new batteries at room temperature. Hence according to the battery circuit model, R2 and R3 do not exist in the circuit model. Using simple circuit equation, R1 values can be calculated by treating the measured 12.9V as the open circuit voltage E. The calculated values of R1 are plotted against the SOD in Fig. 5 at various discharge current levels.

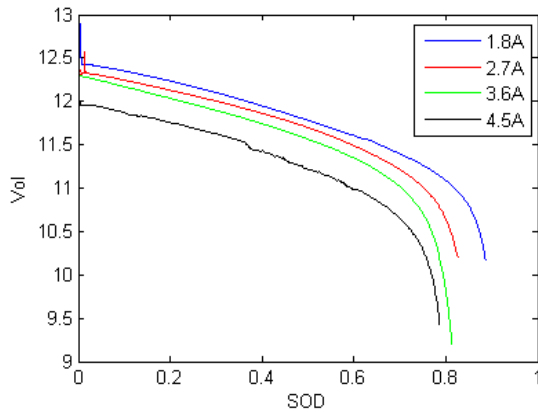


Fig. 4. Voltage profiles at selected constant discharge current levels: at ambient temperature 25 °C

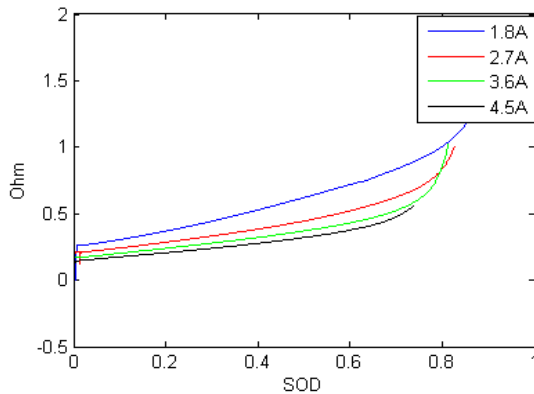


Fig. 5. R1 at selected discharging current levels plotted against SOD at 25 °C ambient

### 5.1.2 R2 tests: discharge at various temperatures

Fig. 6 shows the results of discharge tests performed at selected ambient temperatures. Due to space constraint, the results of tests at the same set of temperatures but for different discharge current levels have not been included in this paper. From these results, it is observed that there are two main impacts of temperature on the battery discharge. First, the capacity of the batteries, *i.e.*, battery SOD at the instance of battery reaching the cut-off voltage of 10.5 V, will decrease as the temperature reduces. Furthermore, a temperature which is higher than the room temperature will cause an increase in the voltage drop at the beginning of the battery discharging. The battery capacity as measured at the time of battery cut-off is also larger.

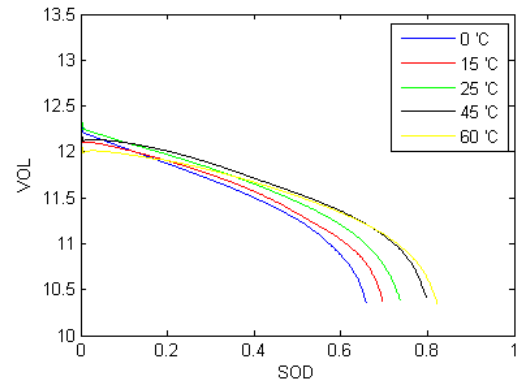


Fig. 6. Discharging curves at various temperatures and at 4.5 A constant discharging current.

With these results, R2 can be calculated and the results are summarized in Fig. 7. As shown, the values of R2 over the range  $0 < \text{SOD} < 0.6$  are quite small compared to that of R1. The negative value of R2 is because the effective value of the battery resistance at temperature higher than 25 °C is lower than that of a brand-new battery operating at 25°C. Hence, a negative value in R2 is to account for this lower resistance value. Also, from the temperature data obtained from on-site WTG stations, it was discovered that the batteries in the stations operated at temperature higher than the test-room ambient temperature of 25°C most of the time. So, it is concluded that the reduction in the battery discharge capacity due to the lower operating temperature can be ignored in practice. For these reasons, R2 has been ignored in the subsequent modeling of the battery. Instead, the impact of temperature on battery age during floating-charge will be considered, as shown in the next section.

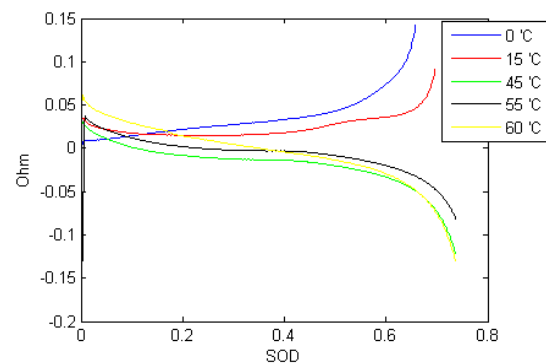


Fig. 7. R2 at selected temperatures with constant discharging current of 4.5A

### 5.2 Analysis of R3 tests: effect on battery age

The tests carried out to determine R3 shall be in accordance to the following two discharge modes: Constant current discharge mode and Initial Large Discharge Current mode.

- Under the constant current discharge mode, the battery will discharge at the constant current level of 4.5 A.
- Under the Initial Large Discharge Current (ILDC) mode, the battery will discharge at 10A

for the first 30 seconds and then the discharge current will revert back to 4.5 A. This mode of discharge reflects more closely the actual discharge duty imposed on the battery in a WTG.

As stated in Section 4, one of the three brand-new batteries was placed in the temperature chamber under floating-charge mode for a number of weeks. The above tests were then performed on the battery after each week of the accelerated aging, until the battery had been aged to the extent that it was unable to maintain the terminal voltage above the cut-off value of 10.5 V for at least 30 minutes. This terminating condition was decided on based on the demand of the essential loads in the WTG and the demand was to be met by the battery.

### 5.2.1 Determination of R3: constant discharge current mode

A sample of the constant current discharging curves after the battery has been aged to various levels is shown in Fig. 8. Extensive tests had also been done at other aging weeks and current levels but the results are not shown here due to space constraint.

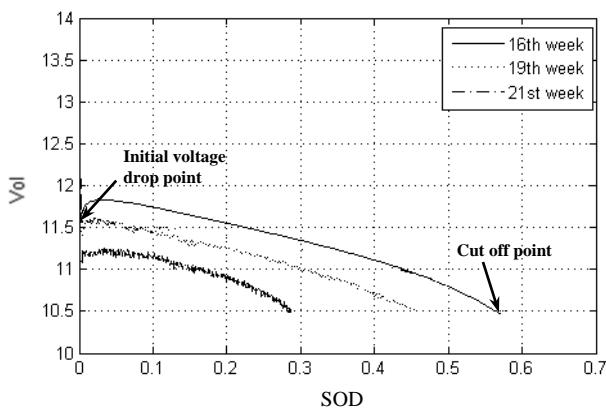


Fig. 8. Discharge curves of battery after accelerated aging of between 16 - 21 weeks at 4.5 A discharge current

Based on these results, a notable observation is that the shapes of all the discharge curves are similar. Essentially the discharge curves are governed by two points: The first (initial) voltage drop and the SOD upon reaching the cut-off voltage. On Fig. 8, these two points are indicated on the discharge curve of the battery after 16 weeks of accelerated aging.

From the preliminary information of a WTG operation, the VRLA batteries used in the WTG are required to discharge at 4.5 A for no less than 30 min. Therefore, the corresponding cut-off SOD can be estimated as  $4.5A \times (0.5hr/6.8 A-h)$  or 0.331, based on the rated battery unit rating of 6.8 A-h. Hence, from Fig. 8, the battery which has been aged for 21 weeks would have seen to have failed to meet this requirement because at the terminating voltage of 10.5 V, the SOD of the battery is approximately 0.29, *i.e.*, less than 0.331. Using (1), by transforming the 21 weeks accelerated aging at 60°C, the equivalent lifetime calculated under 20°C is about 7 years. This value agrees with the

lifetime value shown on the manufacturer data sheet. Also, even with the initial voltage drop, the battery terminal voltage is still some distance above the critical value of 10.5V. Based on this result, it can be concluded that under constant current discharge mode, the battery failure can only be due to the deficiency in the battery capacity. The initial voltage drop will not affect the battery lifetime under this mode of discharge operation.

### 5.2.2 Discharge tests under ILDC mode

Based on information received from the WTG manufacturer, the VRLA batteries in the WTG are more likely to discharge under the Initial Large Discharge Current (ILDC) mode. Hence discharge tests under the ILDC mode were also carried out on all the three battery units. A sample of the results obtained under these tests is shown in Fig. 9.

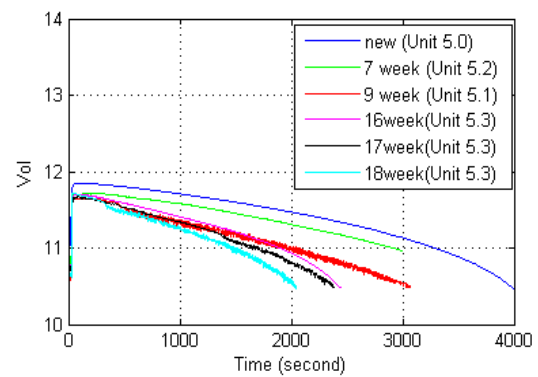


Fig. 9. Discharge curves under ILDC mode: Terminal voltage versus discharge time

When comparing these results with those obtained under constant discharge current mode, it is found that the initial large current discharge causes a larger voltage drop in the first 30-sec or so. As soon as the discharging current is reverted back to the stated constant 4.5 A level, the terminal voltage level recovers to a higher level. However, the overall voltage profile is still lower than that shown under the constant discharge current test at 4.5 A. In fact, under the ILDC mode and based on the criteria of cut-off voltage at 10.5 V, the failure of the battery is seen to have occurred after 9 weeks of accelerated aging. This is much earlier than that when the constant discharge current mode is assumed. The initial voltage in the ILDC mode could reach the critical 10.5V value and when this happens, the battery will end its service life even if the battery VA capacity is still larger than that required to meet the load requirement.

The above tests serve to illustrate the fact that for battery performance prediction, it is necessary to for the tests to emulate as closely as possible the actual discharge pattern in the WTG .

## 6 PROPOSED APPROACH ON LIFETIME PREDICTION

One main finding from the above analysis is that a relatively large voltage drop will occur at the beginning

of the discharge when a battery operates under the ILDC mode. For this reason, battery performance obtained from the constant current discharge tests cannot be applied directly to the situation when the battery operates under the ILDC conditions.

In this section, an approach to predict battery performance and hence its lifetime is presented. To illustrate this approach, the battery performance prediction based on the constant discharge current test data is discussed first.

### 6.1 Performance prediction

Fig. 8 shows the discharge curves of the VRLA battery at a constant discharge current and after the battery has been aged to various levels. It is seen that the capacity of the battery to meet the load demand decreases with the increase in the battery age. The capacity is evaluated at the instant when the battery terminal voltage reaches the cut-off level of 10.5V. Hence, the general trend of the battery performance degradation is clear. It can also be seen that the shapes of all the discharging curves are fairly similar. As stated under Section 5.2.1, the discharging curves can be characterized by two points: The first (initial) voltage drop and the terminating SOD at the cut-off voltage, as shown in Fig. 8. One may attempt to construct a general discharging curve to describe any other discharge condition based on these two values. Unfortunately, due to the inevitable measurement errors, sometime the results of the discharge tests on batteries of very similar age can lead to inconsistency. So the battery lifetime prediction could be inaccurate if one uses these test results directly. Instead, it is proposed a sample of several discharge test curves be used to derive the general discharge curve, so as to minimize the effect of the measurement errors. From the selected curves, the values of the initial voltage drop and terminating SOD at cut-off were extracted and shown in Table 1.

To describe the discharging curves at any battery age, the “polyfit” algorithm in MatLab was used to derive the empirical equations to relate the number of weeks of aging ( $x$ ) with the initial voltage drop ( $y_1$ ) and the battery terminating SOD ( $y_2$ ) at the cut-off voltage. Based on the data given in Table 1, the “polyfit” algorithm provides the following best-fit equations for  $y_1$  and  $y_2$ :

$$y_1 = -0.0028x^2 - 0.0269x + 12.2259; \quad (4)$$

$$y_2 = -0.0005x^2 - 0.0142x + 0.8353. \quad (5)$$

From (4) and (5), discharge curves can be generated for given  $x$  and a sample of them is as shown in Table 2. Using the selected reference curves and the respective  $y_1$  and  $y_2$  values, similar curve-fitting exercise could also be done to obtain the polynomial expression relating the battery terminal voltage ( $V$ ) and battery SOD. The curve-fitting assumes that the open-circuit voltage  $E$  is constant during discharge. For example, the best-fit polynomial obtained for a battery after 3 weeks of aging is

$$V(\text{SOD}) = -30.39 \times \text{SOD}^5 + 48.89 \times \text{SOD}^4 - 27.4 \times \text{SOD}^3 + 4.91 \times \text{SOD}^2 - 1.13 \times \text{SOD} + 12.15. \quad (6)$$

Curves for other aged battery can be obtained in similar manner.

Duration of battery aging	Initial voltage value ( $y_1$ )	Terminating SOD at 10.5 V ( $y_2$ )
0 week (New)	12.22	0.8353
3 weeks	12.12	0.7885
7 weeks	11.9	0.7132
11 weeks	11.59	0.6232

Table 1 Values of  $y_1$  and  $y_2$  obtained from the selected discharge curves

Duration of accelerated age	Initial voltage drop ( $y_1$ )	Terminating SOD at Cut-off voltage ( $y_2$ )
2 weeks	12.1609	0.8049
4 weeks	12.0735	0.7705
6 weeks	11.9637	0.7321
8 weeks	11.8315	0.6897
10 weeks	11.6769	0.6433
12 weeks	11.4999	0.5929

Table 2 Values of  $y_1$  and  $y_2$  obtained from (4) and (5)

The predicted discharge curve can be compared to the discharge curve obtained from tests. The comparison is shown in Fig. 10 for the battery aged after 4 weeks. Similar comparison has also been done for various battery accelerated ages and it is seen that the maximum error in the voltage prediction is within 3% over the whole SOD range. Accuracy of this magnitude is deemed acceptable for most engineering applications. Therefore, it is proposed that the empirically obtained or predicted discharge curves be used for battery lifetime prediction and for the determination of the parameters incorporated in the battery circuit model.

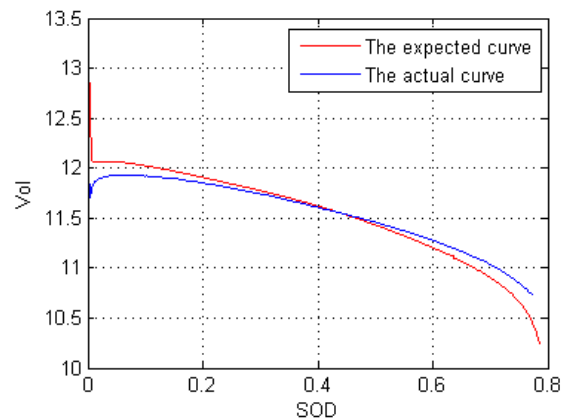


Fig. 10. Comparison between the predicted and actual discharge: 4-week accelerated aging.

### 6.2 Predicted lifetime of the VRLA battery

Section 5.2.1 states that for the VRLA battery to operate successfully on a WTG, the terminating SOD should be more than 0.331 on the battery rating of 6.8 A-h. Also based on the test results, under the constant

current discharge mode, the initial voltage drop will remain almost constant. Therefore, the main cause of battery failure in this case would be due to the inadequacy in its capacity to deliver energy. Hence only the SOD at the cut-off point should be focused on. By substituting  $y_2 = 0.331$  into equation (5), the lifetime of the battery is predicted to be 20.5885 weeks at the accelerated age under 60°C ambient temperature floating-charge. Based on the VRLA lifetime calculation equation described by (1), the predicted lifetime at the reference ambient temperature of 20°C is  $20.5885 \times 2^{((60-20)/10)}$  or 6.33 years. This result agrees very well with the constant discharge current test results described in Section 5.2.1 and also that stated in the manufacturer's data sheet. It suggests that if the actual battery charge/discharge mode at the WTG can be incorporated into the charge/discharge tests, the test data can be used to construct the empirical discharge curve in the way described earlier. The predicted lifetime of the battery can be determined.

As described in Sections 3 and 5, the battery lifetime model based on performance can work independently from the circuit model approach. Hence a software tool has been developed by the authors based on the method described in the sections.

## 7 CONCLUSIONS AND RECOMMENDATIONS

An approach to predict the lifetime of a particular type of VRLA has been proposed. It is based on extracting from the results of an extensive series of tests and the construction of a circuit model to predict the performance of the battery during discharge. From the results of the aging tests conducted so far, the predicted battery service lifetime values under floating-charge appear to agree very well with that stated by the manufacturer. It provides the authors with confidence in using the developed soft tool in predicting the VRLA battery lifetime when temperature is the dominant stress factor.

In the course of the investigation, it was discovered that the ILDC mode would cause a relatively larger initial voltage drop at the beginning of the discharge than that during constant discharge current. Hence, the battery performance prediction model cannot be applied directly on the ILDC using the data obtained from the aging tests. As the lifetime of batteries could be significantly reduced when it is discharged in the ILDC mode, it may be possible to extend the lifetime by changing the discharge mode closer to the constant current discharge mode through a re-scheduling of the WTG essential load demand. This possibility can be explored once a clearer understanding of the back-up power demand of the WTG has been obtained.

Other areas for future work could include the effect of charging method on the battery lifetime as it has been known that batteries under floating-charge using different types of charger do show differences in performance. Finally, it remains unclear if the proposed approach can be applied to other lead-acid batteries of

different manufacture. This would require additional verification studies.

## REFERENCES

- [1] H. Wenzla, I. Baring-Gould, R. Kaiser, B. Y. Liaw, P. Lundsager, J. Manwell, A. Ruddell, and V. Svoboda, "Life prediction of batteries for selecting the technically most suitable and cost effective battery", *J of Power Sources* 144 (2005), pp. 373–384.
- [2] V. Svoboda, "Definition of performance requirements for energy storage systems in each category of use", project funded in part by the European Union, ENK6-CT2001-80576. <http://www.benchmarking.eu.org/>.
- [3] H. Bindner, T. Cronin, P. Lundsager, J. F. Manwell, U. Abdulwahid and I. Baring-Gould, "Lifetime modeling of lead acid batteries", April 2005, *Risø-R-1515(EN)*, pp. 13-14.
- [4] A. Tenno, R. Tenno, T. Suntio "Charge-discharge behavior of VRLA batteries: model calibration and application for state estimation and failure detection", *J of Power Sources* 103(2001),pp.42-53.
- [5] H. Gu, T.V. Nguyen and R.E. White, "A mathematical model of a lead acid cell: discharge, rest and charge", *J. Electrochem. Soc.* 134 (12) (1987) 2953-2960
- [6] D.M. Bemardi and H. Gu, "Two-dimensional mathematical model of a lead acid cell", *J. Electrochem. Soc.* 140 (8) (1983) 2250-2258
- [7] H. Gu, C.Y. Wang and B.Y. Liaw, "Numerical modeling of coupled electrochemical and transport processes in lead acid cell", *J. Electrochem. Soc.* 144 (6) (1997) 2053-2061
- [8] D. Simonsson, P. Ekdunge and M. Lindgren, "Kinetics of the porous lead electrode in the lead acid cell", *J. Electrochem. Soc.* 135 (7) (1988) 1614-1618
- [9] P. Ekdunge and D. Simonsson, "The discharge behavior of the porous lead electrode in lead acid battery. I. Experimental investigation", *J. Appl. Electrochem.* 19 (1989) 127-135
- [10] D. Berndt, R. Brautigam and U. Teutsch, "Temperature compensation of float voltage, the special situation of VRLA batteries", *Proc. 7<sup>th</sup> Int. Telecom Energy Conf., The Netherlands, 1995*, pp.1-12.
- [11] D. Berndt, "Maintenance-Free Batteries", Research Studies Press Ltd, Wiley, New York.
- [12] T. Tsujikawa, T. Matsushita, K. Yabuta and T. Matsushita, "Estimation of the lifetimes of valve-regulated lead-acid batteries", *J of Power Sources* 187 (2009), pp.613–619.
- [13] VRLA Battery type LC-R127R2PG: <http://www.actec.dk/Panasonic/pdf/LC-R127R2P.pdf>.